Chemical Engineering Science, Vol. 47, No. 4, pp. 721–735, 1992.
Printed in Great Britain.

0009–2509/92 $5.00 + 0.00

NONLINEAR MODEL-PREDICTIVE CONTROL OF DISTRIBUTED-PARAMETER SYSTEMS

ASHUTOSH A. PATWARDHAN, GLENN T. WRIGHT and THOMAS F. EDGAR†
Department of Chemical Engineering, The University of Texas at Austin, Austin, TX 78712, U.S.A.

(*Received for publication 6 August 1991*)

Abstract—This paper describes the application of nonlinear model-predictive control (NMPC) to two distributed-parameter processes. The first system is a packed distillation column. The process gain varies in sign with the reboiler heat duty due to mass transfer effects. As a result, only a linear controller with gain scheduling can successfully control the process, but this prevents the outputs from settling to a steady state. The change in the sign of the gain also implies that there is a maximum achievable separation. NMPC recognizes this limit on the achievable separation, and does not continuously alter the manipulated variables in an attempt to reach an unrealizable set-point. The second example is a fixed-bed catalytic reactor. Like the packed column, the fixed-bed reactor may require that the control algorithm deal with equilibrium effects that cause the sign of the reactor gain to vary. In addition, the time constants as well as the delay time of the system vary significantly with the gas flow rate. Inverse response may also be exhibited by the system. Because of the wide range of nonlinear effects that these systems exhibit, NMPC is an intuitively appealing approach that appears to be especially well-suited for such processes. In each case NMPC performance is superior to that of traditional linear controllers.

INTRODUCTION

Many of the processes encountered in chemical engineering such as packed columns, fixed-bed reactors and heat exchangers are nonlinear distributed-parameter systems. Traditionally, these systems have been approximated by linear second-order-plus-dead-time models. These simple transfer function models can be used to design linear model based control strategies like internal model control (Garcia and Morari, 1982), model algorithmic control (Richalet *et al.*, 1978), dynamic matrix control (DMC) (Cutler and Ramaker, 1980) and simplified model-predictive control (Arulalan and Deshpande, 1987). Use of these low-order linear models for control is often adequate when the process nonlinearities are mild, and plant operation is constrained to a small region about a nominal steady state.

Successful control of severely nonlinear systems, however, is critically dependent upon knowledge of the nonlinear dynamics of the processes. Nonlinear model based control algorithms can be applied to processes described by a wide variety of model equations, such as nonlinear ordinary differential/algebraic equations, partial differential equations, integro-differential and delay-differential equations. Such models are accurate over a broad range of operating conditions. Model-predictive control strategies based on these nonlinear models allow tight control of the process, improved constraint handling and greater robustness in terms of handling unusual dynamics and time delays. In addition, these control strategies may permit plant operation in a region that is economically attractive, but where a linear controller will not be able to control the process satisfactorily.

There are two ways of performing model-predictive control calculations. The first method employs separate algorithms to solve the differential equations and to carry out the optimization. First, the manipulated variable profile is guessed, and the differential equations are solved numerically to obtain the controlled variable profile. The objective function is then calculated. The gradient of the objective function with respect to the manipulated variable can be found either by numerical perturbation or by solving sensitivity equations. The control profile is then updated using some optimization algorithm, and the process repeated until the optimal profiles are obtained. This is a sequential solution and optimization strategy, and recent versions of this strategy have been reported by Asselmeyer (1985), Morshedi (1986), Economou *et al.* (1986), Jang *et al.* (1987), Kiparissides and Georgiou (1987) and Peterson *et al.* (1989). The availability of accurate and efficient integration and optimization packages permits implementation of this method with little programming effort. However, it is difficult to incorporate constraints on state variables into this procedure. Also, the algorithm requires the solution of differential equations at each iteration. Jones and Finch (1984) found that such methods spend about 85% of the time integrating the model equations in order to obtain gradient information. This can make them prohibitive in terms of computation time, and unattractive for use in real-time applications.

An attractive alternative is to use a simultaneous solution and optimization strategy. The model differential equations are discretized, and along with the algebraic model equations are included as constraints in a nonlinear programming (NLP) problem posed as

optimize some objective function $F(\mathbf{x}, \mathbf{u})$
such that (1) the (discretized) model differential equations are satisfied, and

† Author to whom correspondence should be addressed.

(2) other constraints (if any) on the states and manipulated variables are met.

In order to keep the dimensionality of the NLP problem low, Hertzberg and Asbjornsen (1977) suggested using orthogonal collocation to discretize the differential equations. A powerful method for solving NLP problems (Edgar and Himmelblau, 1988) is successive quadratic programming (SQP), an infeasible path optimization method. SQP does not require that the constraints be satisfied (the model equations be solved) at each iteration, but finds the optimum and satisfies the constraints simultaneously. Examples of the use of orthogonal collocation in conjunction with SQP to determine open-loop optimal manipulated-variable trajectories have been reported by Biegler (1984), Cuthrell and Biegler (1987) and Renfro *et al.* (1987). This open-loop algorithm is simply an efficient method for solving an optimal-control problem subject to constraints. The obvious disadvantage of using open-loop algorithms for process control is that modeling errors and disturbances cause the process to deviate from the optimal trajectory and produce poor performance.

Patwardhan *et al.* (1988, 1989, 1990) and Eaton and Rawlings (1990) developed NMPC (nonlinear model-predictive control), which extended the method to incorporate feedback. This improved the robustness of the nonlinear control scheme to modeling errors and unmeasured disturbances. Eaton and Rawlings (1990) studied the sensitivity of the NLP to model parameters and control moves. The sensitivity information was useful in determining which model parameters needed to be determined accurately, in studying the effect of the manipulated variables on controller performance, and in the selection of tuning parameters. Patwardhan *et al.* (1990) applied NMPC to the start-up of a nonadiabatic, nonisothermal CSTR, and found it to be robust to errors in model parameters. Eaton and Rawlings (1992) studied model-predictive control of nonminimum phase systems, systems with input constraints, and nonlinear processes with multiple and unstable steady states. Wright and Edgar (1991) investigated the use of NMPC by inverting the steady-state process model to control a water-gas shift reactor.

A similar algorithm was reported by Brengel and Seider (1989), who linearized the nonlinear model differential equations and employed an analytic solution to the linear approximation. The nonlinear differential equations were then replaced by the approximate analytic solution in the NLP. For cases when the set of differential equations were nonstiff, this led to a reduction in the computational effort required to solve the NLP.

The Newton-type control algorithm of Economou (1985) and Economou *et al.* (1986) for unconstrained nonlinear processes was extended to constrained systems by Li and Biegler (1988). This was done by reformulating the control problem using the receding horizon framework. A single-step prediction algorithm was employed, and a SQP strategy was used to address constraints on the process variables. Some stability results were derived for the algorithm. The single-step strategy had limited applicability, and could not be used to control processes when the time delay was larger than the sampling time, or the time delays between different input–output pairs were different. This limitation was removed by the development of a multistep prediction algorithm (Li and Biegler, 1990a), which also improved its robustness characteristics. Results from operator theory were invoked to obtain sufficient stability conditions. The effect of modeling error and measurement noise was investigated, and robust stability conditions were derived (Li and Biegler, 1990b). The use of parameter estimation in conjunction with the nonlinear controller was found to significantly improve closed-loop response when process–model mismatch was present.

THE NMPC ALGORITHM

The simultaneous solution and optimization approach discussed above is applied to the following problem:

$$\min_{\mathbf{u}(t)} \Phi(\mathbf{x}, \mathbf{u}). \tag{1}$$

The process is described by the following differential/algebraic equations:

$$\frac{d\mathbf{x}}{dt} = \mathbf{f}(\mathbf{x}, \mathbf{u}; \mathbf{p}) \tag{2}$$

$$\mathbf{y} = \mathbf{g}(\mathbf{x}, \mathbf{u}; \mathbf{p}) \tag{3}$$

where $\mathbf{y}$ and $\mathbf{u}$ are the controlled- and the manipulated-variable vectors respectively, $\mathbf{x}$ is the state variable vector and $\mathbf{p}$ is the set of model parameters which may include disturbances. Equations (2) and (3) may be replaced by forms that are implicit in $d\mathbf{x}/dt$ and $\mathbf{y}$ respectively. In the examples considered later in this paper Φ is chosen to be the integral square error (ISE). In order to use orthogonal collocation on finite elements, the prediction horizon of V sampling periods corresponds to V finite elements—one element for each sampling period. The control horizon is of U sampling periods. w_j are the weights for a quadrature rule (Villadsen and Stewart, 1967), $\mathbf{x}_{ij}$ is the state vector at the jth collocation point on the ith finite element and u_i is the manipulated variable on the ith finite element. At every sampling instant, $\mathbf{x}_{11}$ is set equal to $\mathbf{x}_{21}$ predicted at the previous sampling instant. If M collocation points (including the two endpoints) are used on each finite element, the NLP problem can be formulated as shown below:

$$\min_{\mathbf{u}} \sum_{i=1}^{V} \sum_{j=1}^{M} \sum_{k=1}^{N} w_j e_{ijk}^2 \tag{4}$$

subject to:

(i) Model differential equations (D contains the

first-derivative weights at the collocation points):

$$\mathbf{D}\begin{bmatrix}\mathbf{x}_{i1}\\ \mathbf{x}_{i2}\\ \vdots\\ \mathbf{x}_{iM}\end{bmatrix}=\begin{bmatrix}\mathbf{f}(\mathbf{x}_{i1},\mathbf{u}_i;\mathbf{p})\\ \mathbf{f}(\mathbf{x}_{i2},\mathbf{u}_i;\mathbf{p})\\ \vdots\\ \mathbf{f}(\mathbf{x}_{iM},\mathbf{u}_i;\mathbf{p})\end{bmatrix},\quad i=1,\ldots,V. \tag{5}$$

Since $\mathbf{x}_{i1}$ is known from the estimator or the previous element, the first equation in eq. (5) is redundant and not used as a constraint.

(ii) Model algebraic equations:

$$\mathbf{y}_{ij}=\mathbf{g}(\mathbf{x}_{ij},\mathbf{u}_i;\mathbf{p}),\quad i=1,\ldots,V;\ j=1,\ldots,M. \tag{6}$$

(iii) Initial condition and continuity of the state variables:

$$\begin{aligned}\mathbf{x}_{11}&=\text{initial condition}\\ \mathbf{x}_{21}&=\mathbf{x}_{1M}\\ &\vdots\\ \mathbf{x}_{V,1}&=\mathbf{x}_{V-1,M}.\end{aligned} \tag{7}$$

(iv) Definition of control horizon:

$$\mathbf{u}_i=\mathbf{u}_{i+1},\quad i=U,\ldots,V-1 \text{ for } V>U. \tag{8}$$

(v) Bounds on state variables:

$$\mathbf{x}_l\leqslant\mathbf{x}_{ij}\leqslant\mathbf{x}_u,\quad i=1,\ldots,V;\ j=1,\ldots,M. \tag{9}$$

(vi) Bounds on the outputs:

$$\mathbf{y}_l\leqslant\mathbf{y}_{ij}\leqslant\mathbf{y}_u,\quad i=1,\ldots,V;\ j=1,\ldots,M. \tag{10}$$

(vii) Bounds on manipulated variables:

$$\mathbf{u}_l\leqslant\mathbf{u}_i\leqslant\mathbf{u}_u,\quad i=1,\ldots,V. \tag{11}$$

(viii) Bounds on changes in the manipulated variables:

$$|\mathbf{u}_i-\mathbf{u}_{i+1}|\leqslant\Delta\mathbf{u}_{\max},\quad i=1,\ldots,U-1. \tag{12}$$

The constrained NLP problem is solved using SQP, and the first manipulated move is implemented. This process is repeated at every sampling instant.

A block diagram of the NMPC structure is shown in Fig. 1 The estimator uses the measured values of the controlled variable, measured disturbances and secondary process measurements to infer the values of the states, and modeled, unmeasured disturbances. The purpose of the dashed line in Fig. 1 is to indicate that the controlled variable may not always be measured explicitly, in which case, its value is inferred by the estimator. In the present example, the effect of modeling error and unmeasured disturbances is treated as an additive, unmeasured disturbance, and is estimated at the nth sampling instant in a manner similar to DMC:

$$\mathbf{y}_{\text{predicted},n}=\mathbf{g}(\mathbf{x},\mathbf{u};\mathbf{p})+\mathbf{d}_{n-1} \tag{13}$$

$$\mathbf{d}_n=\mathbf{y}_{\text{measured},n}-\mathbf{y}_{\text{predicted},n}. \tag{14}$$

This constitutes the feedback portion of the algorithm, which differentiates it from the open-loop, optimal manipulated-variable profile calculation methods of Biegler (1984) and Renfro *et al.* (1987). If a perfect process model is available, $\mathbf{d}$ is equal to the additive disturbance in the process output.

This paper describes the application of NMPC to two simulated distributed-parameter processes. The first system is a packed distillation column. The process gain varies in sign with the reboiler heat duty due to mass transfer effects. As shown in this paper, if a linear controller is used, gain scheduling is required to control the process, but this prevents the outputs from settling to a steady state. The change in the sign of the gain also implies that there is a maximum

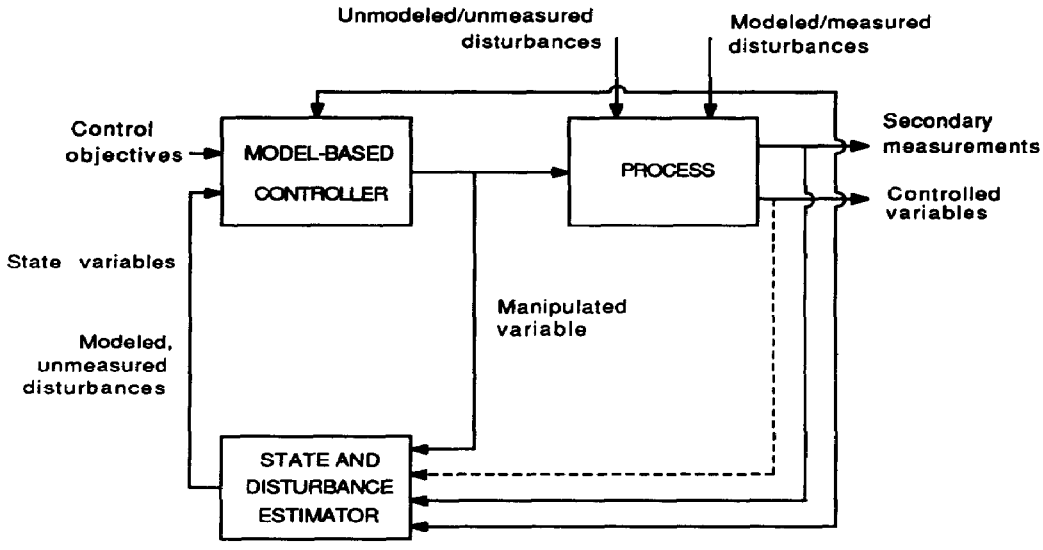

Fig. 1. Structure of the nonlinear model-predictive controller.

achievable separation. NMPC recognizes this limit on the achievable separation, and does not continuously alter the manipulated variables in an attempt to reach an unrealizable set-point. The second example is a fixed-bed catalytic reactor. Like the packed column, the fixed-bed reactor may require that the control algorithm deal with equilibrium effects that cause the sign of the reactor gain to vary. In addition, the time constants as well as the delay time of the system vary significantly with the gas flow rate. Inverse response may also be exhibited by the system. Because of the wide range of nonlinear effects that these systems exhibit, NMPC is an intuitively appealing approach that appears to be especially well-suited for such processes. In each case NMPC performance is compared to that of traditional linear controllers.

EXAMPLE 1: BINARY DISTILLATION IN A PACKED COLUMN

The first example is the control of a packed distillation column separating a mixture of cyclohexane and *n*-heptane at atmospheric pressure. The column contains Sulzer BX structured packing manufactured by Koch Engineering Co. Design data and nominal operating conditions for the column are shown in Table 1. The mole fractions of the light component in the distillate and bottom products are the controlled variables, and are regulated by manipulating the distillate rate and the reboiler duty. The feed flow rate and feed composition are uncontrolled disturbances which tend to drive the controlled variables away from their set-points.

The distillation column exhibits some interesting nonlinearities. Bravo *et al.* (1990) reported that the wetting characteristics of a packing have a strong influence on its efficiency, as well as on the response of the column to different operating conditions. Figure 2 shows the steady-state bottoms composition as a function of the reboiler heat duty. At high feed rates, the separation achieved by the column increases with the reboiler heat duty. At lower feed rates, however, the opposite trend is seen, which is contrary to normal

Table 1. Design and nominal operating data for the packed column

Pressure	1 atm ($\alpha = 1.687$)
Column cross-sectional area (A)	0.144 m^2
Height of rectifying section (Z_R)	3 m
Height of stripping section (Z_S)	3 m
Reflux drum holdup (υ_{drum})	0.07 m^3
Sump holdup (υ_{sump})	0.15 m^3
Reboiler holdup (υ_{reb})	0.07 m^3
Light component	cyclohexane
Heavy component	*n*-heptane
Feed flow rate (F)	1.5 gmol/s
Feed thermal condition	saturated liquid
Mole fraction of light component in the feed (z_F)	0.5
Distillate flow rate (D)	0.75 gmol/s
Mole fraction of light component in the distillate (x_D)	0.9727
Mole fraction of light component in the bottoms (x_B)	0.0273
Reboiler duty (Q_{reb})	1.3×10^5 W
Packing	Sulzer BX†

†For Sulzer BX at atmospheric pressure, $k_y^0 a_m = 72.207 \times 10^{5.6782 V/A}$.

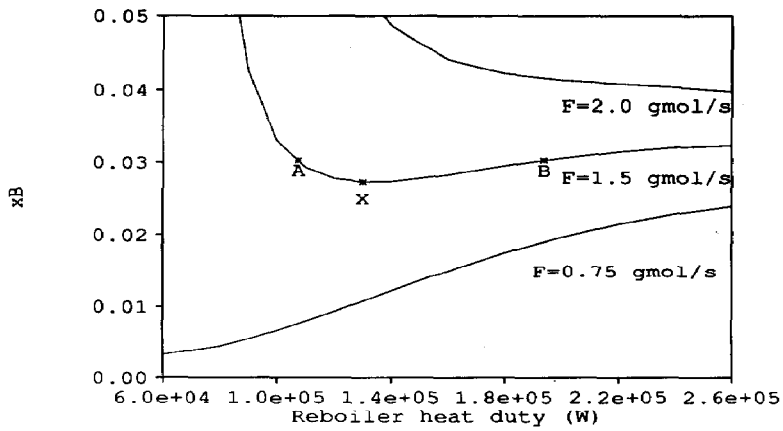

Fig. 2. Steady-state bottoms composition versus reboiler heat duty.

expectation. At intermediate feed rates, the separation reaches a maximum and then decreases, and the location of this maximum varies with the feed rate. These different types of behavior are observed in a region where the reflux ratio is fairly high (moderate- to high-purity products) and are, therefore, likely to be encountered during normal operation. This behavior has important implications for control.

It can be seen from Fig. 2 that, for $F = 1.5$ gmol/s and $z = 0.5$, there are some (x_D, x_B) set-point pairs that are infeasible. For example, $x_D = 0.9757$ and $x_B = 0.0243$ $(= 1 - x_D)$ require that $D = 0.75$ gmol/s, but Fig. 2 shows that for this combination of F, D and z, there is no Q_R that will drive x_D to 0.9757 and x_B to 0.0243. It is also evident from Fig. 2 that two different values of Q_R can produce identical product compositions. The points marked A and B in Fig. 2 correspond to the same F, z, D, x_D and x_B, but different Q_R. Furthermore, for a given F, z and D, there is a maximum separation the column can achieve, which is marked by $\times$.

Figure 2 also shows that the process gain between the reboiler heat duty and the top and bottom product compositions can change sign as the reboiler duty is varied. This implies that a linear controller cannot be used to control the distillation column. For example, suppose that the column is operating at the point $\times$ in Fig. 2. If the plant is perturbed slightly, a linear controller will be able to bring the outputs back to their set-points only as long as the process gain at the perturbed point and the controller gain have the same sign. In addition, moderate changes in the feed rate can cause the column to switch between different behaviors. If the feed rate increases from the value at $\times$, the product compositions can no longer be maintained at the set-point, because the maximum separation that can be achieved at the new feed rate is less than the separation at $\times$. A linear controller would constantly alter the manipulated variables until they saturated in an attempt to bring the outputs to their set-points. This problem can be overcome to some extent by switching the sign of the controller gain as the process gain changes sign, but this can cause the outputs to oscillate without reaching a steady state.

The dynamic behavior of the distillation column was simulated using model Q from Patwardhan and Edgar (1989). However, this detailed model is not suitable for use in NMPC calculations. An NMPC formulation [eqs (1)–(12)] using this model would generate an NLP containing a large number of variables and constraint equations. Such an NLP would require a large amount of CPU time for its solution at each sampling instant. This would create a large delay between sampling and implementation of the control moves, and, in the extreme case, the calculation time would be larger than the sampling time. Therefore, a simpler model which contains fewer equations and states must be used in the controller calculations. Appendix A describes the packed-column model used in NMPC calculations.

Results

We compared the performance of NMPC with DMC (Cutler and Ramaker, 1980) *via* simulation for control of the packed distillation column. The tuning parameters for NMPC and DMC are shown in Table 2. With DMC, no constraints were imposed on either the inputs or the outputs. Note that we used two collocation points on each finite element, which is the same as using backward finite differences to evaluate the time derivatives. This produced satisfactory results in our example, but in general, it may be necessary to use $M > 2$. The NLP was solved using NPSOL (Gill *et al.*, 1986). Step-tests on the plant model yielded the following model for DMC:

$$\begin{bmatrix} \Delta x_D(s) \\ \Delta x_B(s) \end{bmatrix} = \begin{bmatrix} \dfrac{-0.56e^{-160s}}{1265s+1} & \dfrac{3.4\times10^{-7}e^{-151s}}{374s+1} \\ \dfrac{-0.63e^{-180s}}{1750s+1} & \dfrac{-3.32\times10^{-7}e^{-563s}}{1830s+1} \end{bmatrix} \begin{bmatrix} \dfrac{\Delta D(s)}{\Delta Q_{reb}(s)} \end{bmatrix}. \quad (15)$$

Table 2. NMPC and DMC tuning parameters for example 1

Parameter	DMC	NMPC
Sampling time (T)	5 min	5 min
Prediction horizon (V)	5	5
Control horizon (U)	1	1
Model horizon	75	—
Collocation points per finite element (M)	—	2
Move suppression parameter	0	—
Weight on x_D in ISE	1	Variables were scaled. No
Weight on x_B in ISE	30	separate weights were added.
Maximum $\lvert\Delta D\rvert$	—	0.25 gmol/s
Maximum $\lvert\Delta V\rvert$	—	1 gmol/s

When $Q_{reb} > 1.3 \times 10^5$ W, the signs of the gains in the second column are switched.

Case I: *set-point change to a feasible operating point.* Figure 3 shows the response of the column when the set-point is changed from the current feasible operating point to a different feasible operating point. The x_D set-point is decreased by 0.003 mole fraction, and the x_B set-point is increased by 0.003. NMPC is seen to take the column to the set-point much faster than DMC. Note that, while the steady-state compositions and distillate rates are the same with NMPC and DMC, the reboiler duties are different. This is a result of the nonlinearity illustrated in Fig. 2, where the points A and B correspond to the same distillate and bottoms compositions, but with different reboiler heat duties. By including the vapor boilup rate with a suitable weight in the objective function, it would be possible to force NMPC to reach steady state at the same Q_R as DMC.

Case II: *set-point change to an infeasible operating point.* Due to modeling error and the presence of unmeasured disturbances, it may not be possible to determine *a priori* if the desired set-point is feasible. If the set-point is infeasible, the controller should maintain the outputs as close to the set-point as possible, without constantly changing the manipulated variable in an attempt to reach the set-point. The x_D and x_B set-points were increased and decreased, respectively, by 0.003 from their nominal values. Since $z_F = 0.5$, and $x_D^{set} = 1 - x_B^{set}$, the distillate rate at steady state must be equal to $0.5F$. However, Fig. 2 shows that there is no value of Q_{reb} for which this can be achieved. DMC takes the process to a region where the process and controller gains have opposite signs, and this causes the reboiler duty to be increased till it saturates. One way to overcome this problem is to switch the sign of the DMC controller gain when $Q_{reb} > 1.3 \times 10^5$. However, this causes the inputs and outputs to oscillate without settling down (Fig. 4). NMPC, on the other hand, recognizes that the set-point is unrealizable, and quickly reaches a steady state. If there was no modeling error, then we would have $x_D = 1 - x_B$ at steady state for the ISE to be minimized. However, since the prediction of x_D and x_B is in error, and the errors are unequal, the ISE is larger than the theoretical minimum. This is because NMPC estimates unequal values for the disturbances in x_D and x_B in eq. (14). The steady-state deviation from set-point could be altered by changing the relative weights on x_D^{set} and x_B^{set}. In the work reported here, the NLP variables were scaled to be close to unity, but no additional weight was imposed on the set-points. If the set-point is feasible, as in case I, NMPC takes the process to its set-point in spite of unequal prediction errors. It should be noted that, although the new set-point is an infeasible operating point, the NMPC NLP always terminates at a feasible point.

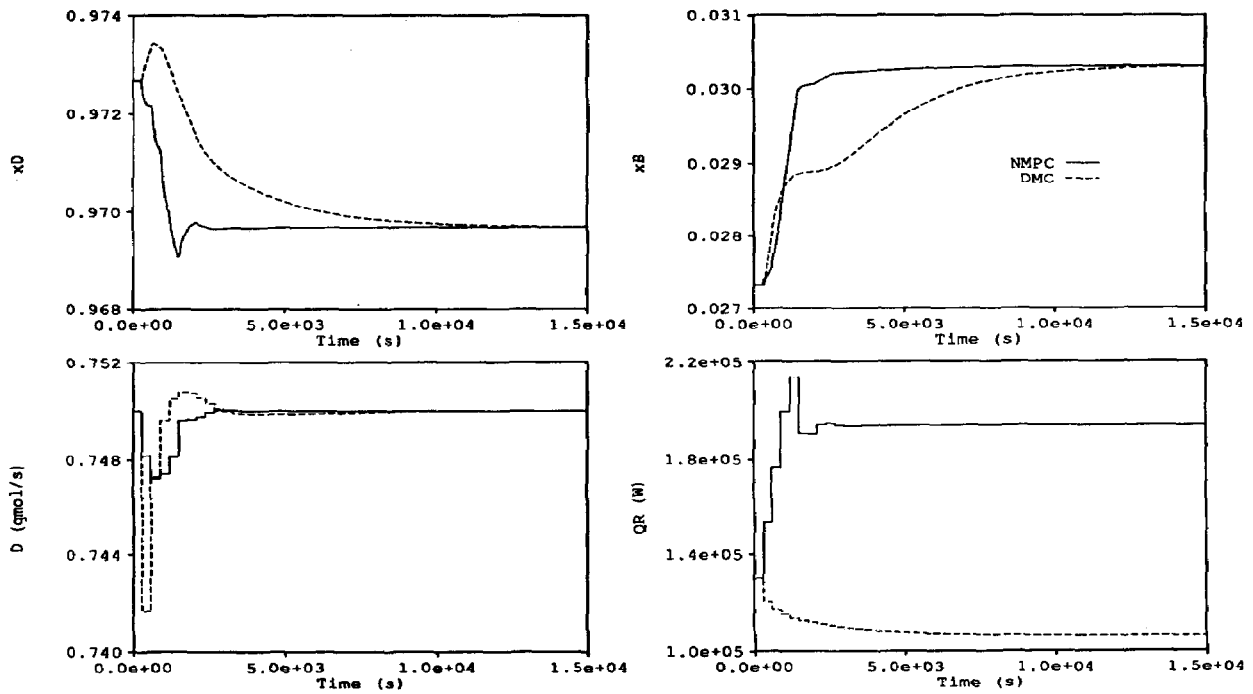

Fig. 3. Packed distillation: comparison of NMPC and DMC for a set-point change to a feasible operating point: (– – – –) DMC; (———) NMPC.

Case III: *step-increase in feed rate.* The response of NMPC and DMC to a step-change in the feed rate from 1.5 gmol/s to 1.65 gmol/s is shown in Fig. 5. This makes the current set-point infeasible. DMC, in an attempt to bring the outputs back to their set-points, increases the reboiler heat duty to a value greater than 1.3×10^5 W. This causes the controller gain (for Q_{reb}) to change sign at the next sampling instant, which in

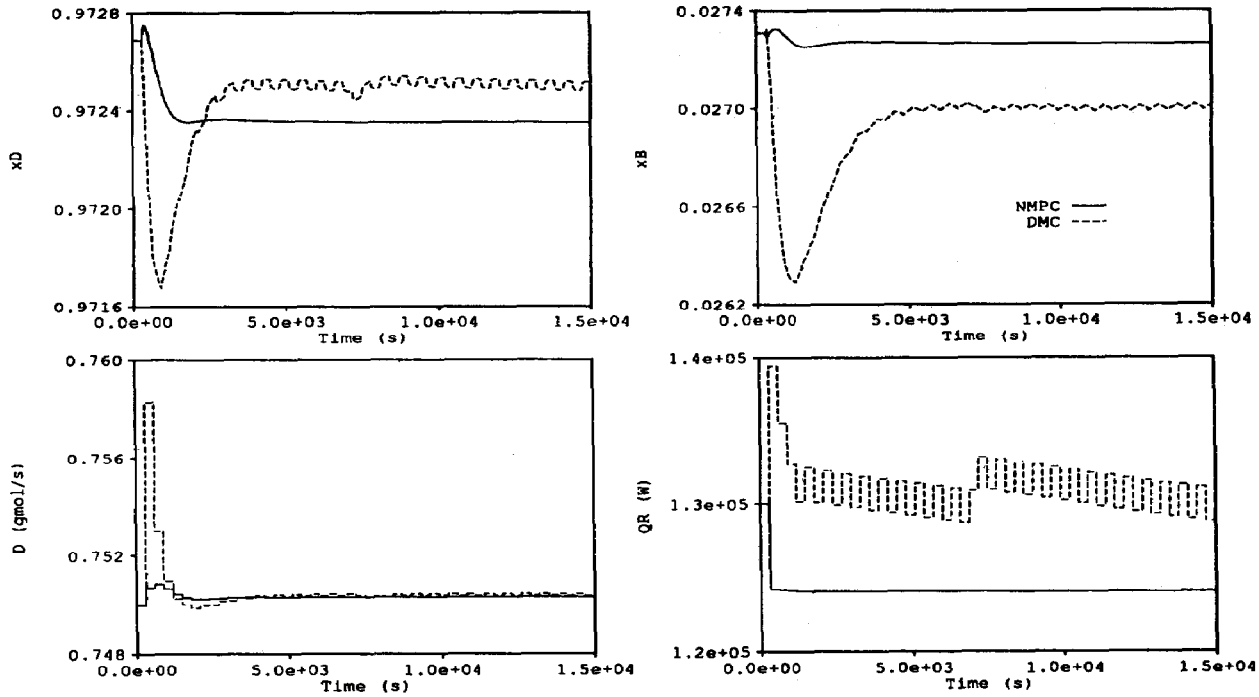

Fig. 4. Packed distillation: comparison of NMPC and DMC for a set-point change to an infeasible operating point: (– – – –) DMC; (———) NMPC.

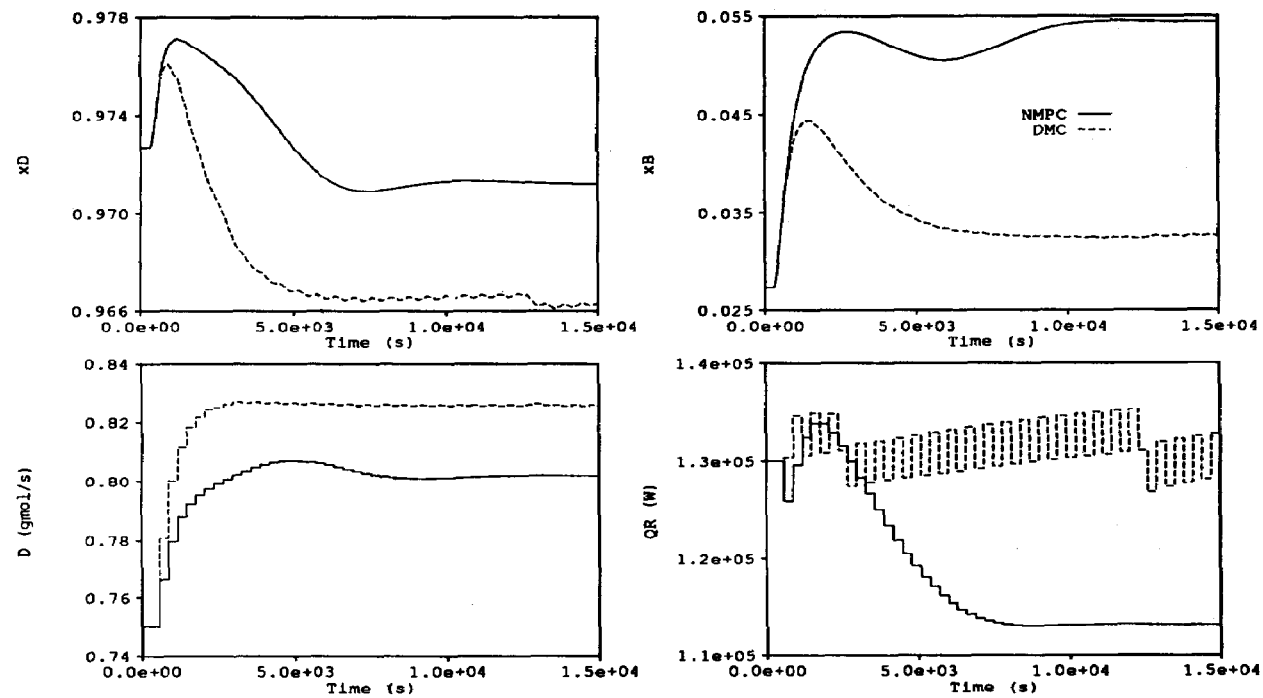

Fig. 5. Packed distillation: comparison of NMPC and DMC for a step-increase in feed rate which makes the current set-point infeasible: (– – – –) DMC; (———) NMPC.

turn makes Q_{reb} less than 1.3×10^5 W. This pattern repeats itself continuously, and causes the manipulated variable to "ring". NMPC, on the other hand, merely attempts to bring the outputs as close to the set-point as possible, and having done this, quickly settles to a steady state. The final deviation from set-point for x_D is greater with DMC, while for x_B NMPC produces the larger deviation from set-point. This is a function of the relative weights on the x_D and x_B set-points in the objective function. These weights can be altered to adjust the relative speed of response for x_D and x_B, and, in cases where the set-point is infeasible, the relative steady-state offset.

Case IV: *NMPC with feed-forward.* The feed rate to the distillation column can be measured without undue difficulty, and this information can be supplied to NMPC for quicker rejection of disturbances in the feed rate. The feed flow rate is a parameter in the controller model used by NMPC, and can be updated according to the available measurement. Thus, feed-forward action is accomplished by updating a model parameter rather than by using a convolution model as in DMC. When the measured feed rate is fed forward to the NMPC controller, Fig. 6 shows that the maximum deviation of the outputs from the set-points is reduced significantly compared to NMPC without feed-forward. While this feed-forward action does not cause the set-point to become feasible, it reduces the modeling error, which causes the outputs to be significantly closer to the set-points at steady state than without feed-forward (case III). During the simulation for case IV, the average CPU time required for NMPC calculations at each sampling instant was 7.2 s on a VAX 3200 computer. The minimum was 2.0 s, and the maximum was 22.3 s. These CPU times are also representative of cases I–III. These times are much smaller than the sampling interval of 5 min, which indicates that the control problem can be solved quickly enough for on-line implementation.

EXAMPLE 2: FIXED-BED WATER-GAS SHIFT REACTOR

The water-gas shift (WGS) reaction, shown below, is reversible and mildly exothermic.

$$CO(g) + H_2O \leftrightarrow CO_2(g) + H_2(g)$$

$$\Delta H_{rxn} = -9.8 \text{ kcal/mol.}$$

In typical industrial applications, the dry process feed contains carbon monoxide, hydrogen, small quantities of hydrocarbons, and sulfur impurities. The reaction is run in either a single adiabatic fixed-bed reactor or in multiple reactors in series when high conversion of carbon monoxide is required. The reactor facility simulated in this study is catalyzed by an iron oxide WGS catalyst. The dry gas feed components (CO, CO_2, and H_2) are supplied by pressure-regulated cylinders. The flow rate of each component is adjusted via a mass flow controller, one associated with each gas. The steam flow rate is regulated by a computer-controlled metering pump. Total gas flow

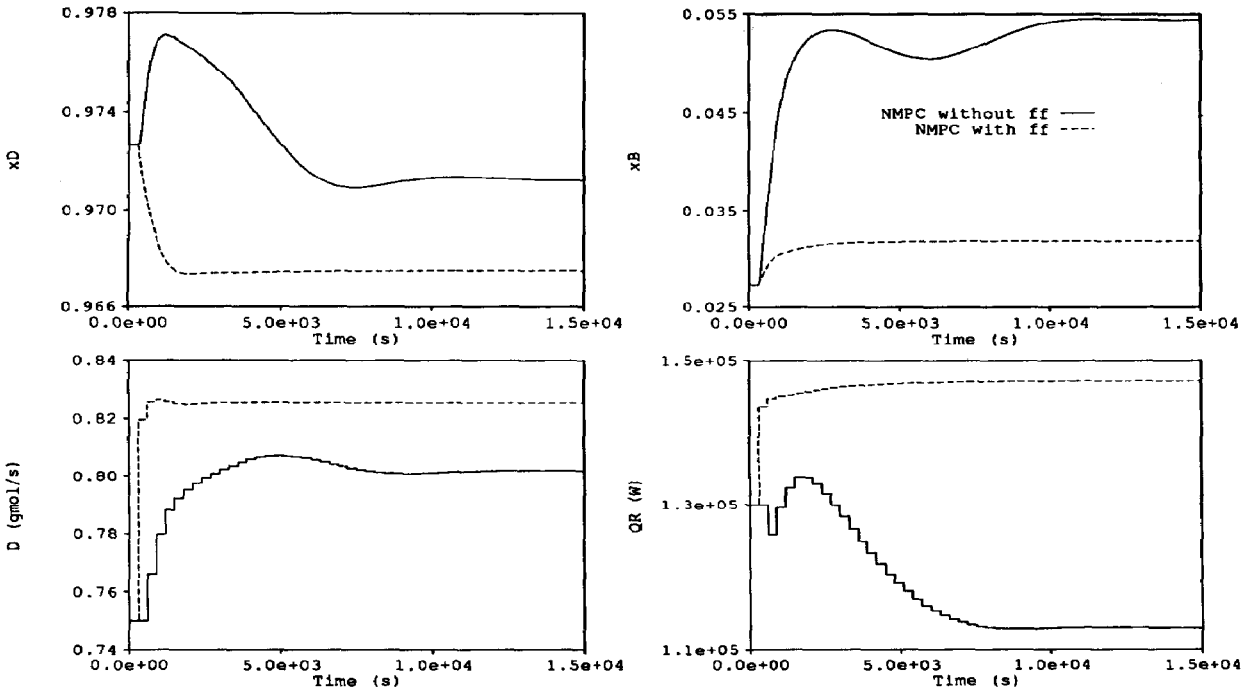

Fig. 6. Packed distillation: comparison of NMPC with and without feed-forward for a step-increase in feed rate which makes the current set-point infeasible: (———) NMPC without feed-forward; (– – –) NMPC with feed-forward.

rates range from 12 to 25 standard liters per minute (SLPM). A WGS reactor model developed by Bell (1990) for a similar system constitutes the real plant in all simulations that follow. Nominal operating conditions and reactor specifications are given in Table 3.

The control objective is to regulate the effluent dry gas composition or the CO conversion. One measure of the effluent composition is the H_2/CO ratio, which is taken to be the controlled variable. The manipulated variables are steam flow rate and power to the inlet heater, given as a fraction of the total available power. For the purpose of regulation under sustained or repeated disturbances, the control system was constructed to return the steam flow rate to its nominal value. This prevents control-input saturation. Steam flow rate is an especially important manipulated variable since it has an immediate impact on the exit composition, while the effects of the inlet heater must slowly propagate through the reactor bed. The control strategy implemented here is similar to that proposed by Wallman *et al.* (1979).

The plant model has several interesting nonlinearities which make linear control unsuitable under many circumstances. Figure 7 illustrates how the steady-state H_2/CO ratio varies with steam flow rate at a nominal power setting of 25%. The diagram clearly indicates that steady-state gain varies substantially and, in fact, changes sign at 6 SLPM where convection starts to dominate the process. Similar behavior is observed when the H_2/CO ratio is plotted against fractional power at a nominal steam flow rate of 5.5 SLPM as illustrated by Fig. 8. When the excess heat in the reactor causes the reverse reaction to dominate the forward reaction, the sign of the gain again changes.

Figure 9 is a plot of the curves in the input space where the steady-state gains change sign for both input variables. Curve A corresponds to the power input, and curve B corresponds to the steam flow rate. In region 1, the gain of the H_2/CO ratio to power is negative and the gain of the H_2/CO ratio to steam flow rate is positive. In region 3, the opposite applies, and in region 2 both gains are positive. While often it is possible to achieve a specific H_2/CO ratio in more than one region, from an economic point of view, it is generally most desirable to operate in region 2 where minimal steam and power are required. Operation in region 1 requires excess energy to drive the reverse reaction in order to achieve the desired H_2/CO ratio, whereas operation in region 3 requires excess steam to generate a convection-dominated process, which limits reaction by reducing the residence time.

Table 3. Design and nominal operating data for WGS reactor

Pressure	1.37 atm
Reactor diameter	1.5 cm
Reactor length	35.6 cm
Bed void fraction	0.3
CO feed flow rate	3.5 SLPM
CO_2 feed flow rate	2.0 SLPM
H_2 feed flow rate	4.0 SLPM
H_2O feed flow rate	5.5 SLPM
Fractional power of inlet heater	0.25
Inlet temperature	573 K
Effluent H_2/CO ratio	4.0463

The primary disturbances to the reactor are fluctuations in the feed temperature and variations in dry gas feed composition and flow rate. A small decrease in the inlet temperature causes the curves in Fig. 9 to shift upward without substantially changing their shapes while a decrease in the inlet temperature has the opposite effect. Small increases and decreases in the dry gas flow rate shift the curves left and right, respectively, and changes in dry gas composition may alter the shape of the curves entirely. Hence, it is easy to demonstrate that relatively small disturbances will result in an unstable closed loop control system when linear control is used unless the inputs are severely restricted. When inputs are restricted in this way, however, their usefulness as inputs is diminished as they will be always saturated.

Controller models

The simulations which follow compare the performance of the nonadaptive generalized predictive

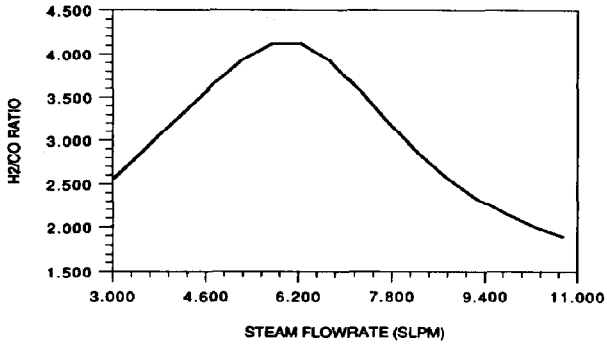

Fig. 7. H_2/CO ratio as a function of steam flow rate for nominal power, dry-gas composition and temperature.

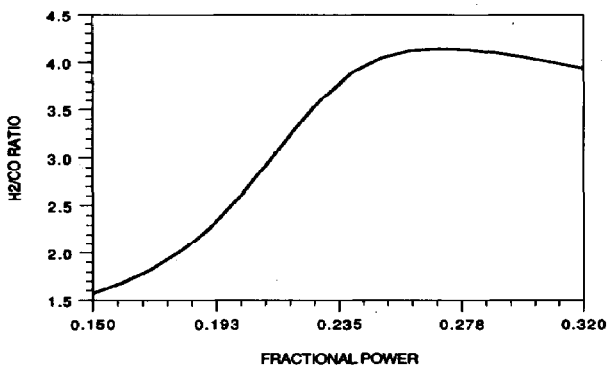

Fig. 8. H_2/CO ratio as a function of fractional power for nominal steam flow rate, dry-gas composition and temperature.

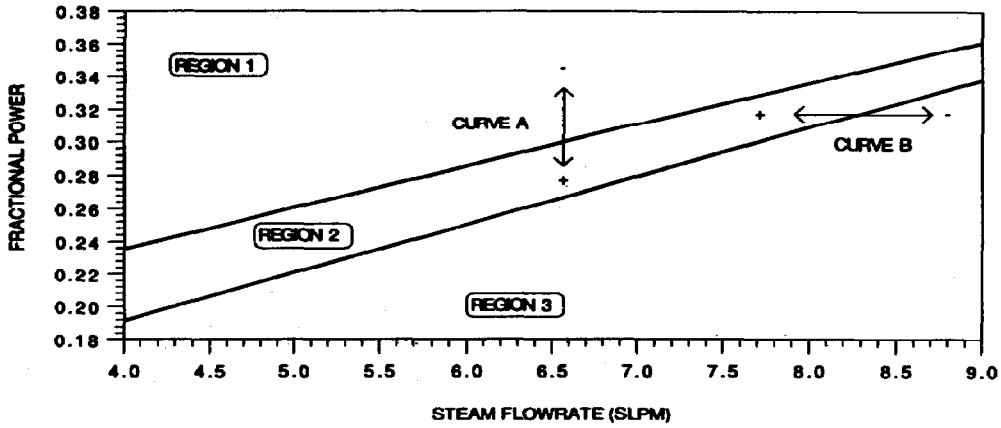

Fig. 9. Operating regions for WGS reactor for nominal dry-gas composition and temperature.

Table 4. Tuning parameters for NMPC and GPC for example 2

Parameter	GPC	NMPC
Sampling time (T)	3 min	6 min
Prediction horizon (V)	15	3
Control horizon (U)	1	1
Collocation points per finite element temporally (M)	—	3
Collocation points spatially	—	5
Move suppression factor	0	—
Weight on H_2/CO in ISE	3	3
Weight on steam flow rate in ISE	1	1

controller (GPC: Clarke *et al.*, 1987) to that of the nonlinear model-predictive controller when applied to the WGS reactor. When the plant model is linearized about the nominal operating point given in Table 3 the following transfer function matrix is obtained:

$$\begin{bmatrix} y_{H_2/CO}(s) \\ u_{steam}(s) \end{bmatrix} = \begin{bmatrix} \dfrac{10.87e^{-0.72s}}{56.28s^2 + 9.57s + 1} & \dfrac{64.46s^2 + 9.02s + 0.364}{103.47s^2 + 15.26s + 1} \\ 0 & 1 \end{bmatrix} \begin{bmatrix} u_{power}(s) \\ u_{steam}(s) \end{bmatrix}. \quad (16)$$

This model is employed in all multivariable GPC simulations.

The model used to simulate the WGS reactor is taken from Bell (1990). Although it is a fairly simple model, it is still far too complex to be used in NMPC calculations. Discretization of this model both spatially and temporally would lead to an NLP with a large number of variables and constraints. We, therefore, make a number of assumptions to derive a model with fewer equations and states. Such simplifications lead to a computationally more tractable NLP. The simplified WGS reactor model, given in Appendix B, constitutes the controller model and is used for all NMPC calculations.

Results

In each NMPC simulation, $V = 3$, $U = 1$, $T =$ 6 min, 4 SLPM $\leqslant u_{steam} \leqslant$ 10 SLPM, $0.1 \leqslant u_{power} \leqslant 0.6$. For GPC, $V = 15$, $U = 1$, $T = 3$ min, the move suppression factor was zero, and the H_2/CO ratio prediction errors from set-point were given a weight 3 times greater than the steam flow rate prediction errors from set-point. The weights were distributed in exactly the same fashion for NMPC. It should be noted that NMPC's objective function could easily have been constructed to return the steam flow rate to within a small neighborhood of the steam flow rate set-point. Latitude can be given to NMPC in this regard because it can easily handle excursions into regions 1 and 3 of Fig. 9, and this added flexibility would allow for a quicker response. While one could certainly allow GPC a similar freedom by not requiring a steam flow rate set-point, numerous simulations have indicated that such freedom leads to instability more often than the scheme proposed here, especially when high conversion is desired or when region 2 is narrow.

Case I: *set-point change to a feasible operating point.* Figure 10 illustrates the response of the reactor

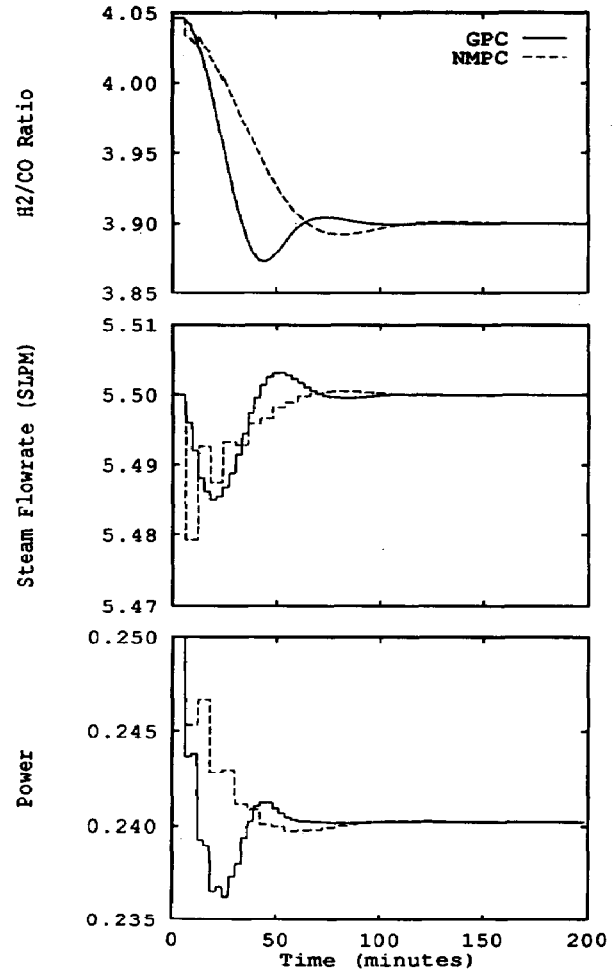

Fig. 10. WGS reactor: comparison of NMPC and GPC for a set-point change to a feasible operating point: (– – – –) NMPC; (———) GPC.

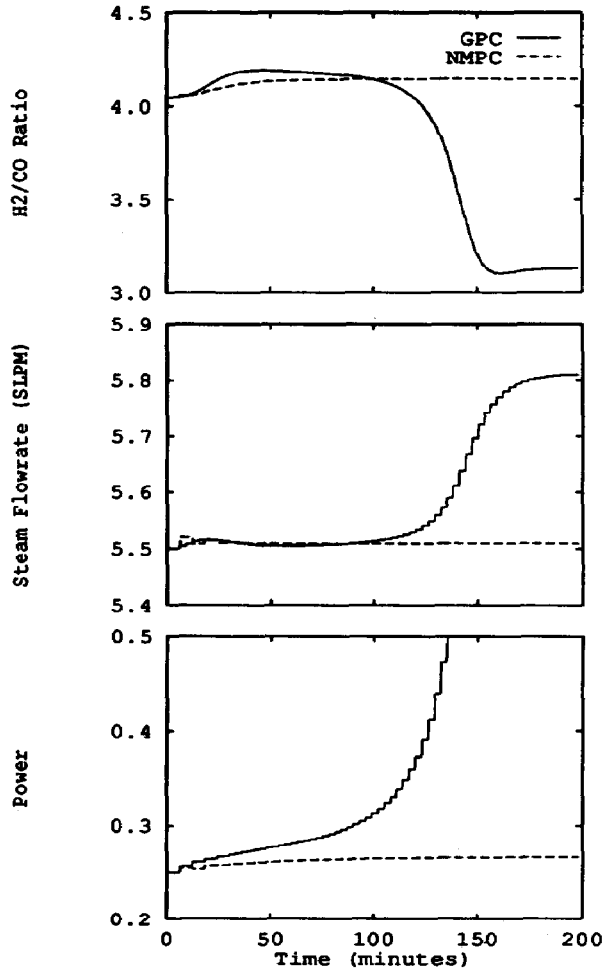

Fig. 11. WGS reactor: comparison of NMPC and GPC for a set-point change to an infeasible operating point: (– – – –) NMPC; (———) GPC.

when the H_2/CO ratio set-point is changed from the nominal operating point to a different feasible operating point near the upper boundary of region 2. The steam flow rate set-point remains unchanged at 5.5 SLPM. Both GPC and NMPC take the reactor to the new set-point with no difficulty. Note, however, that, while the response times are similar, NMPC has considerably less overshoot.

Case II: *set-point change to an infeasible operating point.* The maximum H_2/CO ratio that can be achieved for a steam flow rate of 5.0 SLPM is 4.14 as illustrated by Fig. 7. Figure 11 depicts the reactor response when an H_2/CO ratio of 4.2 is required of NMPC. NMPC recognizes that this set-point is unattainable; it, therefore, moves the effluent composition to the maximum possible H_2/CO ratio and then ceases to vary the inputs. GPC, on the other hand, takes the process into region 1 where the controller and process gain have opposite signs. This quickly results in input saturation.

Case III: *step-increase in inlet temperature.* Both NMPC and GPC successfully reject an inlet temperature disturbance of 15°C as demonstrated in Fig. 12. This is to be expected since changes in inlet temperature can be easily compensated for by appropriately varying the power to the inlet heater. Variations in the inlet temperature constitute a fairly mild disturbance. Note, however, that the response realized when NMPC is used is sluggish in comparison with GPC. This is due, in part, to the fact that GPC has a smaller sampling time. More importantly, however, this disturbance leads to a significant plant–model mismatch for NMPC. While this problem can be overcome easily, in this case, by measuring upstream temperature and supplying it to the model as demonstrated in Fig. 12, often an estimator would be required to achieve good performance with NMPC.

Case IV: *step-change in dry-gas feed flow rate.* Variations in the dry-gas flow rate affect the reactor's behavior differently. Figure 13 shows the

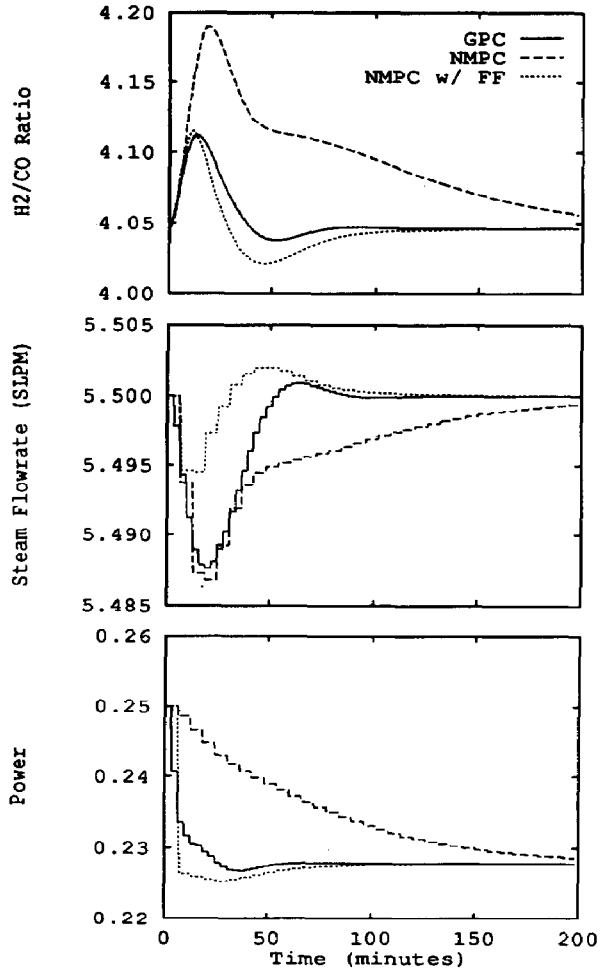

Fig. 12. WGS reactor: comparison of NMPC and GPC for a step-increase in inlet feed temperature: (– – – –) NMPC; (. . . . . .) NMPC with feed-forward; (———) GPC.

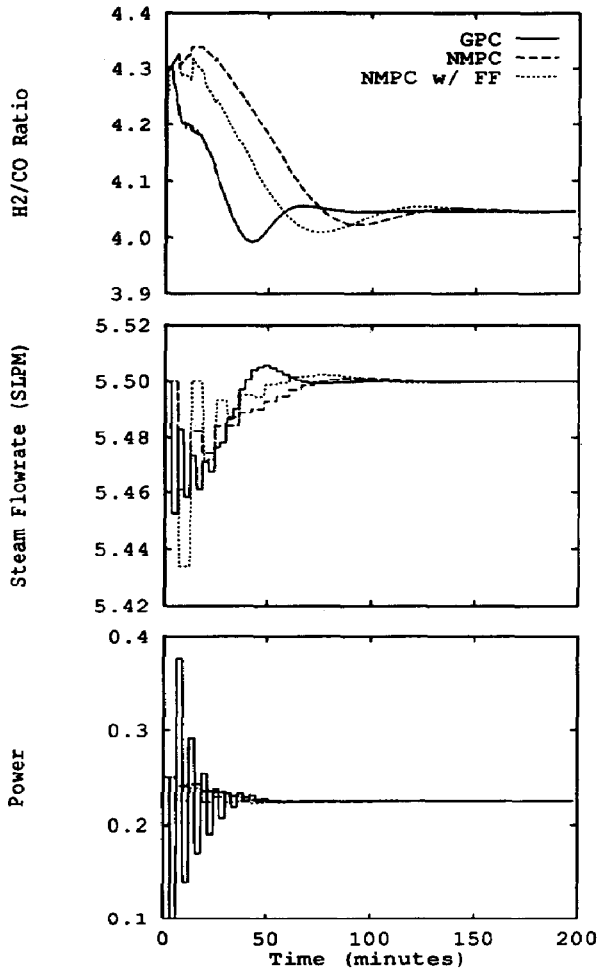

Fig. 13. WGS reactor: comparison of NMPC and GPC for a step-decrease in feed flow rate: (– – – –) NMPC; (. . . . . .) NMPC with feed-forward; (———) GPC.

response of the reactor to a 5% decrease in the dry-gas flow rate. Both GPC and NMPC adequately reject the disturbance, but the linear controller experiences substantial ringing in the power input, which is undesirable. Ringing could be removed at the expense of response time by sufficiently detuning the controller. This suggests, however, that optimal performance can be achieved only with several controller parameter sets. When a 5% increase is made in the dry-gas flow rate, GPC fails to reject the disturbance and saturates the inputs. This occurs because a 5% increase in the dry-gas flow rate moves the plant into an infeasible region where the input constraints are violated. While NMPC encounters the same obstacle, it moves the plant to an optimal operating point in a least-squares sense.

CONCLUSIONS

This paper demonstrated, *via* simulation, the control of two distributed-parameter systems using nonlinear model-predictive control. For control of the packed distillation column, the NMPC controller used a simplified, ordinary differential equation model to describe the dynamics of the distributed-parameter system, and for the WGS reactor, the NMPC controller employed a simplified PDE/ODE equation set. NMPC proved to be robust to these errors in model structure. The process gain changed sign in the region of operation for both the distillation column and the fixed-bed reactor. NMPC was able to recognize this, and provided good control even when the set-point was changed to an infeasible value, or when a disturbance made the current set-point infeasible. Incorporating feed-forward further improved NMPC's performance by reducing plant–model mismatch. A linear controller (DMC) with gain-scheduling was unable to control the distillation column satisfactorily, and exhibited "bang-bang" behavior when the set-point became infeasible. Similarly, GPC saturated the control inputs when the set-point for the WGS reactor became infeasible. It should be noted that these drawbacks are inherent in all linear controllers, and are not

limited to DMC and GPC. These examples illustrate that NMPC can provide good control for highly nonlinear processes. It may permit process operation in regions that are economically attractive, but which are avoided at present because a linear controller is unable to make the process run smoothly and safely in these operating regions.

Experimental verification of the simulation results reported in this paper is in progress.

Acknowledgements—The first author acknowledges support from NSF Grant CBTE-8420001, the Eastman Kodak Company and the Separations Research Program at the University of Texas at Austin. The second author acknowledges support from the Ford Foundation.

NOTATION FOR NMPC FORMULATION

D	matrix containing first-derivative weights at the collocation points
d	vector of disturbance estimates
$\mathbf{e}_{ijk}$	error between the set-point and the controlled variable
f	model differential equations
g	model algebraic equations
M	number of collocation points on each finite element
N	number of outputs
p	vector of model parameters
T	sampling time
t	time
U	control horizon
u	vector of manipulated variables
V	prediction horizon
w	integration weights at the collocation points
x	vector of state variables
y	vector of outputs

Subscripts

i	finite element
j	collocation point
k	output
n	sampling instant
l	lower bound
u	upper bound

Superscript

set	set point

NOTATION FOR EXAMPLE 1: PACKED DISTILLATION

A	cross-sectional area of the column, m^2
a_m	interfacial area for mass transfer, m^2/m^3
D	distillate rate, gmol/s
F	feed rate, gmol/s
K_y^0	overall mass transfer coefficient in the vapor film at zero flux, gmol $m^{-2} s^{-1}$/mole fraction
L	liquid flow rate, gmol/s
Q_{reb}	reboiler heat duty, W
s	Laplace transform variable
t	time, s
V	vapor flow rate, gmol/s
x	mole fraction of the light component in the bulk liquid phase
y	mole fraction of the light component in the bulk vapor phase
Z	height of packed section, m
z	mole fraction of light component in the feed

Greek letters

α	relative volatility
μ	parameter in eqs (A2) and (A3)
Ξ	parameter in eqs (A2) and (A3)
ρ	molar density, $gmol/m^3$
σ	parameter in eqs (A2) and (A3)
υ	holdup, m^3
Ω	parameter in eqs (A2) and (A3)

Subscripts

1	top of the rectifying section
2	top of the stripping section
3	bottom of the stripping section
4	sump
B	bottom product
D	distillate
drum	reflux drum
L	liquid phase
R	rectifying section
reb	reboiler
S	stripping section
sump	sump at the bottom of the column
V	vapor phase

Superscript

–	stripping section

NOTATION FOR EXAMPLE 2: WGS REACTOR

c_{P_g}	gas heat capacity in active bed, cal/gm/K
Da	Damköhler number
ΔH_{rxn}	heat of reaction, cal/gmol
Le	Lewis number
Pe	axial Peclet number
$(-r_{CO})$	reaction rate of carbon monoxide, gmol CO $cm^{-3} s^{-1}$
St	Stanton number for CSTR model of reactor inlet
S	dimensionless heat generation term
T	dimensionless reactor bed temperature
t	dimensionless time
W	CO weight fraction
z	dimensionless axial position

Greek letters

β	thermal Damköhler number
ξ_j	dimensionless constants for CSTR model of reactor inlet

Subscripts

c	CSTR model of reactor inlet
i	inlet to reactor
h	heat

REFERENCES

Asselmeyer, B., 1985, Optimal control for nonlinear systems calculated with small computers. *J. Optimization Theory Applic.* **45**, 533.

Arulalan, G. R. and Deshpande, P. B., 1987, Simplified model predictive control. *Ind. Engng Chem. Res.* **26**, 347.

Bell, N. H., 1990, Steady-state and dynamic modeling of a fixed-bed water-gas shift reactor. Ph.D. dissertation, The University of Texas at Austin, TX.

Bequette, B. W., 1986, Measurement selection and control system design for multivariable interacting processes. Ph.D. dissertation, The University of Texas at Austin, TX.

Biegler, L., 1984, Solution of dynamic optimization problems by successive quadratic programming and orthogonal collocation. *Comput. chem. Engng* **8**, 243.

Bravo, J. L., Patwardhan, A. A. and Edgar, T. F., 1990, Influence of effective interfacial areas in the operation and control of packed distillation columns. Paper No. 37a, A.I.Ch.E. Spring National Meeting, Orlando, Florida.

Brengel, D. D. and Seider, W. E., 1989, Multistep nonlinear predictive control. *Ind. Engng Chem. Res.* **28**, 1812.

Clarke, D. W., Mohtadi, C. and Tuffs, P. S., 1987a, Generalized predictive control—I. The basic algorithm. *Automatica* **23**, 137–148.

Clarke, D. W., Mohtadi, C. and Tuffs, P. S., 1987b, Generalized predictive control—II. Extensions and interpretations. *Automatica* **23**, 159–160.

Cuthrell, J. E. and Biegler, L. T., 1987, On the optimization of differential/algebraic process systems. *A.I.Ch.E. J.* **33**, 1257.

Cutler, C. R. and Ramaker, B. L., 1980, Dynamic matrix control—a computer control algorithm. Joint Automatic Control Conference Proceedings, Paper WP-5B.

Eaton, J. W. and Rawlings, J. B., 1990, Feedback control of chemical processes using on-line optimization techniques. *Comput. chem. Engng* **14**, 469–479.

Eaton, J. W. and Rawlings, J. B., 1992, Model-predictive control of chemical processes. *Chem. Engng Sci.* **47**, 705–720.

Economou, C. G., 1985, Operator theory approach to nonlinear controller design. PhD thesis, California Institute of Technology, Pasadena, CA.

Economou, C. G., Morari, M. and Palsson, B. O., 1986, Internal model control. 5. Extension to nonlinear systems. *Ind. Engng Chem. Process Des. Dev.* **25**, 403.

Edgar, T. F. and Himmelblau, D. H., 1988, *Optimization of Chemical Processes*, Chap. 8. McGraw-Hill, New York.

García, C. E. and Morari, M., 1982, Internal model control 1. A unifying review and some new results. *Ind. Engng Chem. Process Des. Dev.* **21**, 308.

Gill, P. E., Murray, W., Saunders, M. A. and Wright, M. H., 1986, User's guide for NPSOL (version 4.0): a fortran package for nonlinear programming. Technical Report SOL 86-2, Systems Optimization Laboratory, Department of Operations Research, Stanford University, California.

Hertzberg, T. and Asbjornsen, O. A., 1977, Parameter estimation in nonlinear differential equations, in *Computer Applications in the Analysis of Data and Plants*. Science Press, Princeton.

Jang, S., Joseph, B. and Mukai, H., 1987, On-line optimization of constrained multivariable processes. *A.I.Ch.E. J.* **33**, 26.

Jones, D. I. and Finch, J. W., 1984, Comparison of optimization algorithms. *Int. J. Control* **40**, 747.

Kiparissides, C. and Georgiou, A., 1987, Finite-element solution of nonlinear optimal control problems with a quadratic performance index. *Comput. chem. Engng* **11**, 77.

Li, W. C. and Biegler, L. T., 1988, Process control strategies for constrained nonlinear systems. *Ind. Engng Chem. Res.* **27**, 1421–1433.

Li, W. C. and Biegler, L. T., 1990a, Multistep, Newton-type control strategies for constrained, nonlinear processes. *Chem. Engng Res. Dev.* **67**, 562–577.

Li, W. C. and Biegler, L. T., 1990b, Newton-type controllers for constrained nonlinear processes with uncertainty. *Ind. Engng Chem. Res.* **29**, 1647–1657.

Morshedi, A. M., 1986, Universal dynamic matrix control. Session VI, Paper No. 2, Chemical Control Conference III, Asilomar, California.

Patwardhan, A. A. and Edgar, T. F., 1989, Dynamics of packed columns with low holdups. Paper No. 35a, A.I.Ch.E. Spring National Meeting, Houston, Texas.

Patwardhan, A. A., Rawlings, J. B. and Edgar, T. F., 1988, Model predictive control of nonlinear processes in the presence of constraints. Presented at the A.I.Ch.E. Annual Meeting, Washington, DC.

Patwardhan, A. A., Rawlings, J. B. and Edgar, T. F., 1989, Model predictive control of nonlinear processes in the presence of constraints, in *IFAC/IEEE Symposium on Nonlinear Control Systems Design* (Edited by A. Isidori), pp. 456–460. Pergamon Press, Oxford.

Patwardhan, A. A., Rawlings, J. B. and Edgar, T. F., 1990, Nonlinear model predictive control. *Comput. chem. Engng* **87**, 123–141.

Peterson, T., Hernandez, E., Arkun, Y. and Schork, F. J., 1989, Nonlinear predictive control of a semi-batch polymerization reactor by an extended DMC. Paper No. TP4, American Control Conference, Pittsburg, Pennsylvania.

Renfro, J. G., Morshedi, A. M. and Asbjornsen, O. A., 1987, Simultaneous optimization and solution of systems described by differential/algebraic equations. *Comput. chem. Engng* **11**, 503.

Richalet, J., Rault, A., Testud, J. L. and Papon, J., 1978, Model predictive heuristic control: applications to industrial processes. *Automatica* **14**, 413.

Villadsen, J. V. and Stewart, W. E., 1967, Solution of boundary-value problems by orthogonal collocation. *Chem. Engng Sci.* **22**, 1483.

Wallman, P. H., Silva, J. M. and Foss, A. S., 1979, Multivariable integral controls for fixed-bed reactors. *Ind. Engng Chem. Fundam.* **18**, 392.

Wright, G. T. and Edgar, T. F., 1991, Adaptive nonlinear control of a laboratory water-gas shift reactor. Presented at ITAC91, IFAC International Symposium on Intelligent Tuning and Adaptive Control, Singapore.

APPENDIX A: CONTROLLER MODEL FOR THE DISTILLATION COLUMN

Model Q described by Patwardhan and Edgar (1989) contains two partial differential equations and five ordinary differential equations in addition to algebraic equations describing mass transfer and vapor–liquid equilibrium in the packing. When the partial differential equations are discretized in the spatial dimension using orthogonal collocation on finite elements, this reduces to a set of $8N_C + 8$ ordinary differential and algebraic equations, where N_C is the number of collocation points in each packed section. This model was used to simulate the actual distillation column, but contained too many equations and variables for use in NMPC calculations. It was simplified to a form suitable for use by the controller by making the following assumptions:

(i) The mass transfer in the packing is described using an overall vapor-phase mass transfer coefficient instead of individual vapor- and liquid-film mass transfer coefficients.

(ii) The liquid holdup in the packing, being much smaller than that in the reflux drum, sump and reboiler, is neglected. This reduces the partial differential equation model to an ordinary differential equation model, for which an analytical solution is available (Patwardhan and Edgar, 1989).

(iii) The vapor boilup rate ($\bar{V}$) is used as the manipulated variable for controller calculations instead of the reboiler duty (Q_{reb}). This decouples the material and energy balances for the sump and reboiler, and the energy balance equations may be omitted from the controller model. The vapor boilup

rate calculated by NMPC is multiplied by the latent heat of vaporization and this is used as the manipulated variable in the actual plant. This simplification introduces two errors into the controller model. First, the constant of proportionality between the reboiler heat duty and the vapor boilup rate is smaller than the latent heat of vaporization in the actual plant because part of the reboiler heat goes towards heating the liquid from the sump up to the reboiler temperature. In addition, the column response to a change in the vapor boilup rate is much faster than the response to an equivalent change in the reboiler heat duty.

(iv) The values of the reflux drum and reboiler holdups are set equal to zero, and the value of the sump holdup is increased so that it equals the sum of the three actual holdups. This significantly affects the way in which the time constant of the controller model varies in response to disturbances and manipulated variable changes.

(v) The feed is at its dew point (100% vapor), and the reflux is at its bubble point. This is a good assumption because the D–Q_{reb} control scheme is fairly insensitive to changes in the feed and reflux enthalpies (Bequette, 1986).

The resulting controller model equations are listed below. This simplified model, which is used in the NMPC calculations contains just three algebraic and one ordinary differential equation.

(i) Light component mass balance around the packed sections:

$$F z_F + \bar{V} x_4 = D x_1 + L x_3. \tag{A1}$$

(ii) Mass transfer in the rectifying section:

$$\frac{AK_y^0 a_m Z_R}{L} = \Omega_R \ln\left(\frac{x_2 - \mu_R}{x_1 - \mu_R}\right) + \Xi_R \ln\left(\frac{x_2 - \sigma_R}{x_1 - \sigma_R}\right). \tag{A2}$$

(iii) Mass transfer in the stripping section:

$$\frac{AK_y^0 a_m Z_S}{L} = \Omega_S \ln\left(\frac{x_2 - \mu_S}{x_1 - \mu_S}\right) + \Xi_S \ln\left(\frac{x_2 - \sigma_S}{x_3 - \sigma_S}\right). \tag{A3}$$

(iv) Light component mass balance around the sump:

$$(\upsilon_{drum} + \upsilon_{sump} + \upsilon_{reb})\rho_L \frac{dx_4}{dt} = L(x_3 - x_4). \tag{A4}$$

Here, Ω_R, Ξ_R, μ_R and σ_R are functions of L, V, x_1 and α, while Ω_S, Ξ_S, μ_S and σ_S are functions of L, $\bar{V}$, x_3, x_4 and α.

APPENDIX B: CONTROLLER MODEL OF THE WATER-GAS SHIFT REACTOR

The following dynamic model of the WGS reactor is a simplification of a model developed by Bell (1990), which consisted of three PDEs and one ODE. The simplifying assumptions used to derive the model for controller design are given below:

(i) The fixed-bed reactor is assumed to be adiabatic. This obviates the need for Bell's energy balance on the reactor wall. The primary ramification of this assumption is that the simplified model cannot predict hot spots, caused by heat losses to the surroundings, which might occur in the more rigorous model. However, heat effects in the reactor can easily be accounted for if reactor wall temperature measurements are available. In any case, the bed temperature of the reactor should never exceed that predicted by the simplified model as a result of this assumption alone.

(ii) The axial reactor compositions are assumed to be those values which would occur if the dynamic temperature profile of the reactor were, in fact, the steady-state temperature profile. This assumption leads to a linear relation between composition and temperature when diffusion is neglected and the ratio of Da to β is assumed to be constant. The resulting algebraic equation replaces the quasi-steady-state carbon monoxide material balance, a differential equation. The errors introduced by these assumptions are: (1) the simplified model does not exhibit the inverse response in the effluent temperature that typically occurs in the more rigorous model and (2) the response of the simplified model is typically faster than the more rigorous model.

The resulting NMPC controller model consists of only one PDE (compared to three for the more rigorous model), one ODE, and one algebraic equation. The controller model equations are given below:

Energy balance:

$$Le\frac{\partial T}{\partial t} = -\frac{\partial T}{\partial z} + \frac{1}{Pe_h}\frac{\partial^2 T}{\partial z^2} + \beta(-r_{CO}). \tag{B1}$$

Carbon monoxide material balance:

$$W(z) = -\frac{Da}{\beta}[T(z) - T(0)] + W(0). \tag{B2}$$

The dimensionless boundary conditions are:

$$z = 0: \quad \frac{\partial T}{\partial z} = Pe_h(T - T_c), \qquad z = 1: \quad \frac{\partial T}{\partial z} = 0.$$

The energy content of the feed gas is changed by varying the power input to the reactor inlet heater, which consists of a cartridge heater placed in a thermowell that is in direct contact with the inlet process stream. The nonactive reactor inlet is modeled as an ideal CSTR.

Energy balance for reactor inlet:

$$Le_c\xi_1\frac{dT_c}{dt} = \frac{c_{p_{g,i}}}{c_{p_{g,c}}}T_i - T_c - St_1\xi_2(T_c - T_{w,c}) + \xi_{3u}. \tag{B3}$$